International Journal of Fracture (2006) 137:109–120
DOI 10.1007/s10704-005-3076-y

Size sensitivity for the reliability index in stochastic finite element analysis of damage

MIGUEL A. GUTIÉRREZ
Faculty of Aerospace Engineering, Delft University of Technology, P.O. Box 5058, 2600 GB Delft, The Netherlands (E-mail: m.gutierrez@lr.tudelft.nl)

Received 9 August 2005; accepted in revised form 6 September 2005

Abstract. The direct differentiation method is applied to the estimation of statistical size effect behaviour in quasi-brittle solids. The scale factor is included in the finite element model and the autocorrelation function. Particular attention is paid to the proper differentiation of the Nataf transformation, which has been chosen to convert the basic random variables into a set of uncorrelated, standard normal variables. The predictive possibilities of the presented algorithm provide a valuable insight in the actual mechanisms responsible for failure. It can be evaluated to what extent the scale factor sensitivity of the failure probability is influenced by the phenomena related to the material disorder or the deterministic size effect.

Key words: Quasi-brittle material, reliability method, sensitivity, statistical size effect, stochastic finite elements.

1. Introduction

Quasi-brittle solids exhibit a strong dependence of the peak load on a characteristic dimension of the considered body. On one hand the average peak load decreases as the size of the body increases. On the other hand the peak load exhibits a larger spread for small bodies. This behaviour is commonly referred to as size effect and is a matter of structural performance vs. a scale factor (Bažant and Planas, 1998). It therefore provides a preferential environment for the application of design sensitivity algorithms.

The concept of sensitivity is open to several interpretations in a context of reliability analysis (Ditlevsen and Madsen, 1996). On the one hand the sensitivity of (estimates of) the probability of failure with respect to selected design parameters can be evaluated. On the other hand, several techniques for estimation of the probability of failure are gradient-based optimisation algorithms, which require evaluation of the sensitivity with respect to the basic random variables. Among the techniques to evaluate the sensitivity with respect to design parameters, only the direct differentiation method (DDM) (Kleiber et al., 1997) seems to be adequate for solids with material non-linearities. The DDM is essentially based on the application of the implicit function theorem to the non-linear algebraic equations which result from the finite element discretisation. When advanced material models are used the dependence of internal parameters on the design parameters must also be considered. This is of special importance when local loading/unloading conditions depend on global variables, as in gradient-enhanced models.

This paper is focused on the direct evaluation of the sensitivity of the probability of failure of quasi-brittle solids with respect to a scale factor. The probability of failure is first approximated by means of the finite element reliability method for a solid with a random strength field (Gutiérrez and De Borst, 1999, 2000). The scaling factor is then incorporated into the mechanical and probabilistic transformation which govern the mapping between the response of the solid, the random strength and an uncorrelated standard normal space of basic variables. The sensitivity of the β-index with respect to the scale factor is then evaluated by means of the DDM.

2. Size effect in gradient-enhanced quasi-brittle solids

2.1. Deterministic model

A reference solid Ω in plane stress conditions is considered. A scaled solid $\Omega^{(s)}$ is introduced by means of a factor $s \in \mathbb{R}$,

$$\Omega^{(s)} = \{\mathbf{y} \in \mathbb{R}^2 | \mathbf{y} = s\mathbf{x} \text{ with } \mathbf{x} \in \Omega\}. \tag{1}$$

This notation implies that

$$\Omega^{(1)} = \Omega. \tag{2}$$

The behaviour of the scaled solid is, in absence of body forces, governed by the boundary value problem

$$\begin{aligned} &\nabla \cdot \boldsymbol{\sigma} = \mathbf{0} && \text{in } \Omega^{(s)}, \\ &\mathbf{u} = s\, {}^{\tau}\bar{\mathbf{u}}_r && \text{on } \partial\Omega_1^{(s)}, \\ &\boldsymbol{\sigma} \cdot \mathbf{n} = {}^{\tau}\bar{\boldsymbol{\sigma}} && \text{on } \partial\Omega_2^{(s)}, \end{aligned} \tag{3}$$

at each instant τ, where $\boldsymbol{\sigma}$ is the stress tensor, $\mathbf{u}$ is the displacement field, $\partial\Omega_1^{(s)} \cup \partial\Omega_2^{(s)} = \partial\Omega^{(s)}$, $\mathbf{n}$ is the outward normal vector to $\partial\Omega$, ${}^{\tau}\bar{\mathbf{u}}_r$ are the prescribed boundary displacements in the reference solid and ${}^{\tau}\bar{\boldsymbol{\sigma}}$ is the prescribed boundary loading. In a context of quasi-static loading, τ is a parameter that merely orders the succession of events. If a linear elastic stress–strain relation is considered, together with a linear kinematic relation between the strain and displacement fields, it can easily be demonstrated that the stress field that provides a solution to Equation (3) does not depend on the scaling. In other words, the field

$$\boldsymbol{\sigma}: \ \Omega^{(s)} \longrightarrow \mathbb{R}^2 \otimes \mathbb{R}^2 \tag{4}$$

does not depend on s, i.e.,

$$\frac{\partial \boldsymbol{\sigma}}{\partial s} = 0. \tag{5}$$

Additionally, it can be demonstrated that the displacement field

$$\mathbf{u}: \ \Omega^{(s)} \longrightarrow \mathbb{R}^2 \tag{6}$$

satisfies the relation

$$\mathbf{u} = s\mathbf{u}_r, \tag{7}$$

where $\mathbf{u}_r$ is the displacement field corresponding to the solution of Equation (3) in the reference solid Ω.

In quasi-brittle materials the stress–strain relation is not linear. If a damage model is considered, this is expressed as

$$\boldsymbol{\sigma} = (1-\omega)\mathbf{D}\boldsymbol{\varepsilon}, \tag{8}$$

where $\mathbf{D}$ is the elastic constitutive tensor and $\omega \in [0, 1]$ is a damage parameter that is a function of a history parameter κ representing the maximum value reached by a spatially averaged, equivalent measure $\bar{\varepsilon}^{\mathrm{eq}}$ of the deformation tensor. This is formalised by a damage loading function

$$f = \bar{\varepsilon}^{\mathrm{eq}} - \kappa, \tag{9}$$

which thus compares $\bar{\varepsilon}^{\mathrm{eq}}$ and κ and the Kuhn–Tucker conditions

$$\dot{\kappa} \geqslant 0, \quad f(\bar{\varepsilon}^{\mathrm{eq}}, \kappa) \leqslant 0, \quad \dot{\kappa} f(\bar{\varepsilon}^{\mathrm{eq}}, \kappa) = 0. \tag{10}$$

Following Peerlings et al. (1996), the averaged equivalent strain satisfies the boundary value problem

$$\begin{array}{ll} \bar{\varepsilon}^{\mathrm{eq}} - \frac{1}{2} l_s^2 \nabla^2 \bar{\varepsilon}^{\mathrm{eq}} = \varepsilon^{\mathrm{eq}} & \text{in } \Omega^{(s)}, \\ \nabla \bar{\varepsilon}^{\mathrm{eq}} \cdot \mathbf{n} = 0 & \text{on } \partial\Omega^{(s)}, \end{array} \tag{11}$$

where the source term $\varepsilon^{\mathrm{eq}}$ is obtained through any suitable invariant measure of the strain field. The parameter l_s in Equation (11) is referred to as internal length-scale and quantifies the width of the zone in which damage is localised. Since this parameter can be viewed as a material property, it is not scaled by factor s. Consequently, the simultaneous solution of Equations (3) and (8)–(11) will not exhibit the similarity expressed by Equations (4)–(7). This lack of similarity is referred to as *size effect.*

This study is restricted to the case of proportional loading, i.e.,

$$\begin{array}{ll} {}^{\tau}\mathbf{u} = {}^{\tau}\lambda s \hat{\mathbf{u}}_r & \text{on } \partial\Omega_1^{(s)}, \\ {}^{\tau}\boldsymbol{\sigma} = {}^{\tau}\lambda \hat{\boldsymbol{\sigma}} & \text{on } \partial\Omega_2^{(s)}, \end{array} \tag{12}$$

where $\hat{\mathbf{u}}_r$ and $\hat{\boldsymbol{\sigma}}$ are fixed patterns of prescribed displacements and stresses respectively and ${}^{\tau}\lambda$ is a scale factor. Solution of Equations (3) and (8)–(11) is equivalent to finding the processes ${}^{\tau}\mathbf{u}$ and ${}^{\tau}\lambda$. The peak load parameter is then defined as

$$\lambda_{\mathrm{p}} = \max_{\tau > 0} {}^{\tau}\lambda. \tag{13}$$

2.2. Random strength distribution

In damage models it is usual to express the strength as a threshold value κ_0 of the history parameter κ introduced in Equation (9). In heterogeneous solids, this variable is considered to be a random field with a known pointwise probability distribution P_{K_0} and an autocorrelation function ρ that quantifies the decay of the correlation coefficient as the distance between two considered points increases. In this study an

exponential autocorrelation function is considered. Making use of the notation introduced in the previous section, the autocorrelation function of the scaled solid reads

$$\rho^{(s)}(\mathbf{x}_i, \mathbf{x}_j) = \exp\left(-\frac{s\|\mathbf{x}_i - \mathbf{x}_j\|}{l_c}\right), \tag{14}$$

where l_c is referred to as correlation length. Equation (14) also means that the autocorrelation coefficient between any two points of the scaled solid can be found in the reference solid by applying the scaling

$$\rho^{(s)} = \rho^s, \tag{15}$$

where ρ represents the autocorrelation function in the reference body. Notice that l_c can be viewed as a material parameter and it remains the same in both the reference and the scaled domains. The actual value of l_c can be estimated from micromechanical considerations (Baxter and Graham, 2000). Equation (15) introduces a scaling in the statistical behaviour of the body. The probability distribution of any property of the solution to Equations (3) and (8)–(11) and, in particular, the peak load parameter (13) will consequently depend on this scaling. The purpose of this study is to estimate the sensitivity of this probability distribution with respect to the scale factor.

3. Approximation of the peak-load statistics

3.1. Reliability method

The distribution of the peak load is approximated by means of the reliability method. For this purpose a limit state function Z is defined as

$$Z = \Lambda_p - \lambda_0, \tag{16}$$

where Λ_p is a random variable representing the peak load parameter and λ_0 represents a threshold such that the body is in a failure state when it is not reached. The probability of failure is then

$$\begin{aligned} \mathcal{P}_f &= \Pr(Z < 0) \\ &= \int_{z<0} p_Z(\theta)\, \mathrm{d}\theta, \end{aligned} \tag{17}$$

where p_Z is the probability density function of Z. The statistical information is however, only available for the strength field through the probability distribution P_{K_0} and the autocorrelation function (14). In order to evaluate integral (17), the strength field must be discretised into a set of n random variables $\mathbf{V}$ characterised by their marginal probability distribution P_{V_i} and their correlation structure (Gutiérrez and Krenk, 2004). The set $\mathbf{V}$ can be converted for algorithmic convenience into a set of uncorrelated standard normal variables $\mathbf{W}$ through a mapping $\mathbf{T}$. This mapping is conveniently realised by means of Nataf's transformation (Ditlevsen and Madsen, 1996; Liu and Der Kiureghian, 1986). The variables $\mathbf{V}$ are first converted into a set of correlated standard normal variables $\mathbf{C}$ through

$$C_i = \Phi^{-1}(P_{V_i}(V_i)), \tag{18}$$

where Φ is the standard normal cumulative distribution function. Then, the variables $\mathbf{C}$ are converted into the uncorrelated set $\mathbf{W}$ through a linear transformation

$$\mathbf{W} = \mathbf{H}\mathbf{C}, \tag{19}$$

where $\mathbf{H}$ is a matrix related to the correlation of $\mathbf{C}$. Since this correlation is related to the scale factor s, c.f. Equation (14), the mapping $\mathbf{T}$, given by Equations (18) and (19) depends explicitly on this scale factor as well. It can then formally be stated that

$$\mathbf{W} = \mathbf{T}(\mathbf{V}, s). \tag{20}$$

The probability of failure (17) is, after this transformation, recast as

$$\begin{aligned} \mathcal{P}_\mathrm{f} &= \Pr(Z < 0) \\ &= \int_{z(\mathbf{w})<0} \varphi_n(\boldsymbol{\omega})\, \mathrm{d}\boldsymbol{\omega}. \end{aligned} \tag{21}$$

The symbol φ_n in Equation (21) represents the n-variate uncorrelated standard normal probability density function. This integral can be accurately computed by means of Monte Carlo techniques. In the particular case of non-linear material models this could become very time consuming. Alternatively, the surface $z(\mathbf{w}) = 0$ can be approximated by low-order surfaces at selected critical points. The procedure is referred to as first- or second-order reliability method depending on the kind of surfaces (hyperplanes or hyperparaboloids) used for approximation (Ditlevsen and Madsen, 1996; Gutiérrez and Krenk, 2004).

When first-order approximations are used the surface $z(\mathbf{w}) = 0$ is approximated by the hyperplane

$$\bar{z}(\mathbf{w}) = \boldsymbol{\alpha}^\mathrm{T}\mathbf{w} + \beta = 0, \tag{22}$$

where $\|\boldsymbol{\alpha}\| = 1$ and β is the distance from the hyperplane to the origin. The approximation point is chosen as the closest point of $z(\mathbf{w}) = 0$ to the origin. This point, with coordinates $-\beta\boldsymbol{\alpha}$ is referred to as design point or β-point and represents a maximum of the probability density function of $\mathbf{W}$ on $z(\mathbf{w}) = 0$. The β index is referred to as reliability index and the probability of failure is approximated by

$$\mathcal{P}_\mathrm{f} = \Phi(-\beta). \tag{23}$$

The β-point can conveniently be computed by means of an optimisation algorithm (Liu and Der Kiureghian, 1991) based on the gradient of the limit-state function (16) and consequently of the peak load parameter λ_p with respect to the basic variables $\mathbf{w}$.

3.2. Estimation of size sensitivity

The probability of failure is approximated by the β index, according to Equation (23). The sensitivity of this probability with respect to any design parameter and, in particular, to the scale factor s can then be estimated by means of the sensitivity of the β-index. According to Ditlevsen and Madsen (1996) this sensitivity is written as

$$\frac{\mathrm{d}\beta}{\mathrm{d}s} = \frac{1}{\left\| \frac{\partial z}{\partial \mathbf{w}} \right\|} \frac{\partial z}{\partial s}, \tag{24}$$

where it is reminded that z and $\mathbf{w}$ represent the limit-state function and the basic variables, respectively. The term $\partial z/\partial \mathbf{w}$ in Equation (24) is elaborated as

$$\frac{\partial z}{\partial \mathbf{w}} = \frac{\partial \lambda_p}{\partial \mathbf{v}} \frac{\partial \mathbf{v}}{\partial \mathbf{w}}. \tag{25}$$

This term is available from the computation of the β-point with a suitable gradient-based algorithm, as mentioned in Section 3.1, and reflects the dependence of the peak load parameter on the discretised strength $\mathbf{v}$ and that of $\mathbf{v}$ on the standard normal variables $\mathbf{w}$ through the Nataf transformation (20). The term $\partial z/\partial s$ is developed by keeping in mind that λ_p depends on s in both a deterministic sense, c.f. Equations (3) and (8)–(13), as well as a probabilistic sense through the Nataf transformation (20). Making use of the chain rule one obtains

$$\frac{\partial z}{\partial s} = \frac{\partial \lambda_p}{\partial \mathbf{v}} \frac{\partial \mathbf{v}}{\partial s} + \frac{\partial \lambda_p}{\partial s}. \tag{26}$$

The term $\partial \lambda_p/\partial \mathbf{v}$ has already been used in Equation (25) and is available from Gutiérrez and De Borst (1999). The term $\partial \lambda_p/\partial s$ is evaluated with the technique presented in Gutiérrez and De Borst (2003). The elaboration of $\partial \mathbf{v}/\partial s$, which is required to evaluate the dependence of λ_p on the scaling factor s in a probabilistic sense, follows from the differentiation of the Nataf transformation and will be described next.

4. Differentiation of the Nataf transformation

The dependence of $\mathbf{V}$ on s is implicitly stated by Equation (20). For the purpose of the evaluation of $\partial \mathbf{v}/\partial s$ the inverse of Equation (20) is considered,

$$\mathbf{V} = \mathbf{T}^{-1}(\mathbf{W}, s). \tag{27}$$

The components of $\mathbf{V}$ are related to those of $\mathbf{C}$ by the inverse of Equation (18),

$$V_i = P_{V_i}^{-1}(\Phi(C_i)) \tag{28}$$

while $\mathbf{C}$ is related to $\mathbf{W}$ by

$$\mathbf{C} = \mathbf{H}^{-1}\mathbf{W}. \tag{29}$$

The dependence on s is found in the matrix $\mathbf{H}$. Since $\mathbf{C}$ and $\mathbf{W}$ are correlated and uncorrelated standard normal variables respectively, matrix $\mathbf{H}^{-1}$ must fulfill the condition

$$\mathbf{H}^{-1}\mathbf{H}^{-\mathrm{T}} = \mathbf{R}_0, \tag{30}$$

where $\mathbf{R}_0$ is the correlation matrix of $\mathbf{C}$. Matrix $\mathbf{R}_0$ is related to the correlation matrix $\mathbf{R}$ of $\mathbf{V}$ through the expression

$$R_{0ij} = \xi R_{ij}, \tag{31}$$

where ξ is a parameter depending on R_{ij} and the marginal distribution parameters of $\mathbf{V}$. If a midpoint discretisation (Gutiérrez and Krenk, 2004) of the random field is considered, the coefficient R_{ij} is given by expressions (14) and (15) as

$$R_{ij} = \left(\rho(\|\mathbf{x}_i - \mathbf{x}_j\|)\right)^s = \rho_{ij}^s. \tag{32}$$

This introduces the scaling factor s in $\mathbf{R}_0$ through

$$R_{0ij} = \xi(\rho_{ij}^s)\rho_{ij}^s. \tag{33}$$

Substituting terms in Equation (30) and differentiating leads to

$$\left[\frac{\partial}{\partial s}(\mathbf{H}^{-1}\mathbf{H}^{-\mathrm{T}})\right]_{ij} = \left[\frac{\partial}{\partial s}\mathbf{H}^{-1}\mathbf{H}^{-\mathrm{T}} + \mathbf{H}^{-1}\frac{\partial}{\partial s}\mathbf{H}^{-\mathrm{T}}\right]_{ij} = \left(\frac{\partial \xi}{\partial \rho} + \xi\right) s\rho_{ij}^{s-1}. \tag{34}$$

There are several choices possible for matrix $\mathbf{H}$. If it is chosen as the square root of $\mathbf{R}_0^{-1}$, then $\mathbf{H}$ is symmetric and the formulation is simplified. Indeed,

$$\frac{\partial}{\partial s}\mathbf{H}^{-1}\mathbf{H}^{-\mathrm{T}} + \mathbf{H}^{-1}\frac{\partial}{\partial s}\mathbf{H}^{-\mathrm{T}} = 2\mathbf{H}^{-1}\frac{\partial}{\partial s}\mathbf{H}^{-1}. \tag{35}$$

The components of $\partial\mathbf{H}^{-1}/\partial s$ are then given by

$$\left[\frac{\partial}{\partial s}\mathbf{H}^{-1}\right]_{ij} = \frac{1}{2}\left(\frac{\partial \xi}{\partial \rho} + \xi\right) s H_{ik}\rho_{kj}^{s-1}, \tag{36}$$

where repeated indices denote summation. The derivatives $\partial\mathbf{v}/\partial s$ are finally computed from

$$\frac{\partial \mathbf{v}}{\partial s} = \frac{\partial \mathbf{v}}{\partial \mathbf{c}}\frac{\partial \mathbf{c}}{\partial s} = \frac{\partial \mathbf{v}}{\partial \mathbf{c}}\frac{\partial \mathbf{H}^{-1}}{\partial s}\mathbf{w}, \tag{37}$$

where the term $\partial\mathbf{v}/\partial\mathbf{c}$ results from direct differentiation of Equation (28).

5. Numerical simulations

The proposed technique is illustrated by means of the single-edge-notched concrete specimen represented in Figure 1. The specimen is subjected to an axial, tensile loading which is applied through rigid, free-rotating platens. The size of the specimen is governed by the measure d. The Young's modulus has been taken $E = 18\,000$ MPa and $\nu = 0.2$. The damage parameter is related to the history parameter κ through the expression

$$\omega(\kappa, \kappa_0) = \begin{cases} 1 - \frac{\kappa_0}{\kappa}[(1-a) + a\exp(-b(\kappa - \kappa_0))], & \text{if } \kappa > \kappa_0, \\ 0, & \text{otherwise,} \end{cases} \tag{38}$$

where the threshold for damage initiation κ_0 is a random field with a pointwise three-parameter Weibull distribution according to the parameters

$$\begin{aligned} \kappa_0^{\min} &= 1.5 \times 10^{-4}, \\ u &= 2.1 \times 10^{-4}, \\ k &= 2, \end{aligned} \tag{39}$$

and an exponential autocorrelation function, c.f. Equation (14), with three different values for the correlation length, $l_c = 15$, 30 and 60 mm. The parameters $a = 0.96$ and

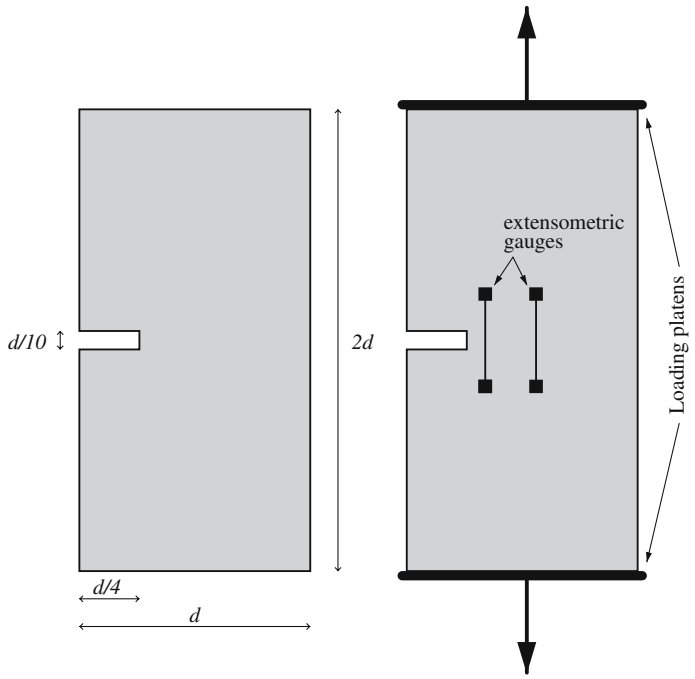

Figure 1. Single-edge-notched specimen: generic geometry and loading conditions.

$b = 350$ represent the relative reduction of the stress as $\kappa \to \infty$ and the rate at which damage grows respectively. This law has been proposed in Peerlings et al. (1998). The equivalent strain ε^{eq} is defined as in De Vree et al. (1996),

$$\varepsilon^{\text{eq}} = \frac{\eta - 1}{2\eta(1-2\nu)} I_1 + \frac{1}{2\eta}\sqrt{\frac{(\eta-1)^2}{(1-2\nu)^2} I_1^2 + \frac{2\eta}{(1+\nu)^2} J_2}. \tag{40}$$

The strain tensor invariants are given by

$$\begin{aligned} I_1 &= \varepsilon_1 + \varepsilon_2 + \varepsilon_3, \\ J_2 &= (\varepsilon_1 - \varepsilon_2)^2 + (\varepsilon_2 - \varepsilon_3)^2 + (\varepsilon_3 - \varepsilon_1)^2, \end{aligned} \tag{41}$$

and the parameter η controls the sensitivity to compression relative to that in tension and is taken $\eta = 10$. This definition of the equivalent strain has been used in Peerlings et al. (1998) to describe concrete structures with a gradient-enhanced damage model. The internal length scale in Equation (11) is $l_s = 4\,\text{mm}$

The specimen, that has a thickness of 50 mm, is discretised into eight-noded, plane-stress finite elements with a 2×2 Gauss–Legendre integration quadrature. The usual servo-control of the loading by the extensometric gauges represented in Figure 1 is simulated with the path-following technique proposed in De Borst (1987). Different sizes have been considered by setting

$$d = s d_r \quad \text{with } s = 1, 1.25, 1.5, 1.75, 2, \tag{42}$$

where $d_r = 100\,\text{mm}$ corresponds to the reference solid. A reference load of 5 500 N has been considered for $s = 1$.

Size effect laws usually relate the size parameter and a normalised nominal stress. With the formulation adopted in this work, the size parameter is directly given by s. The peak loading factor λ defined in Equation (13) can also be viewed as a normalised nominal stress measure. The β-indices computed for each size also take this scaling into account.

The numerical results for β and $d\beta/ds$ are represented in Figure 2. This figure is of a purely illustrative character. Figures 3 and 4 represent the evolution of the contribution of the terms $(\partial\lambda_p/\partial\mathbf{v})(\partial\mathbf{v}/\partial s)$ and $(\partial\lambda_p/\partial s)$, both scaled by $\partial z/\partial\mathbf{w}$ according to Equation (24), which account for the probabilistic and the deterministic dependence of λ_p on s, respectively.

It is readily observed that the probabilistic contribution to the size sensitivity of β is positive while the deterministic contribution is negative. A more relevant observation is, however, that the absolute value of the deterministic contribution is much larger than that of the probabilistic contribution, with a factor up to 250 for the correlation length $l_c = 60\,\text{mm}$ and the scaling factor $s = 1$. This suggests that the sensitivity of the β-index to size variations is essentially introduced by the deterministic size effect for the size range considered.

The conclusion stated above is valid for single β-points. When considering larger or unnotched specimens it can be expected that multiple failure modes will be observed and accordingly several β-points will be present. In that case, the probabilistic contribution to the size sensitivity can be expected to become dominant, in accordance with Weibull law. The evaluation of this sensitivity requires knowledge of that of the correlation coefficient between different failure modes. The latter is based on the second derivatives of the limit-state function with respect to the basic variables (Ditlevsen and Madsen, 1996), which are beyond the scope of this work.

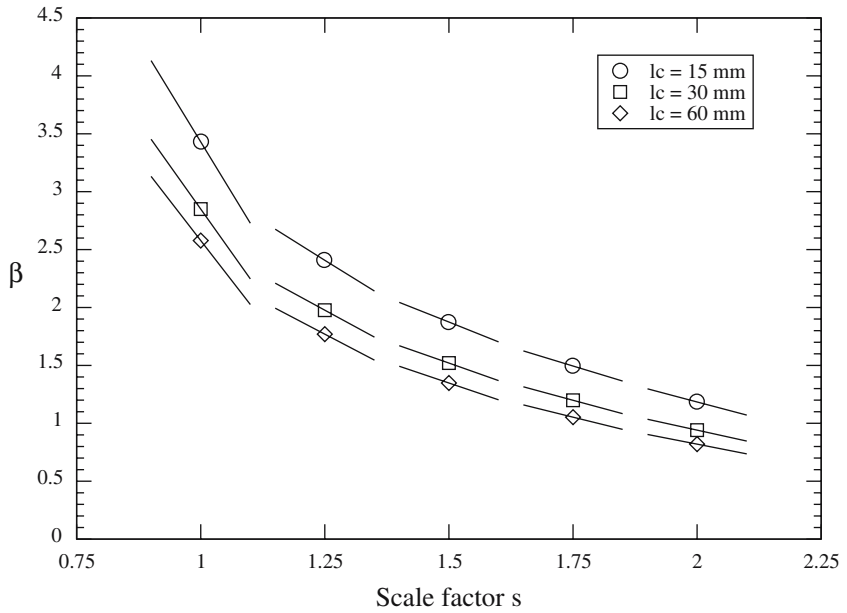

Figure 2. Representation of the numerical results for β and $d\beta/ds$.

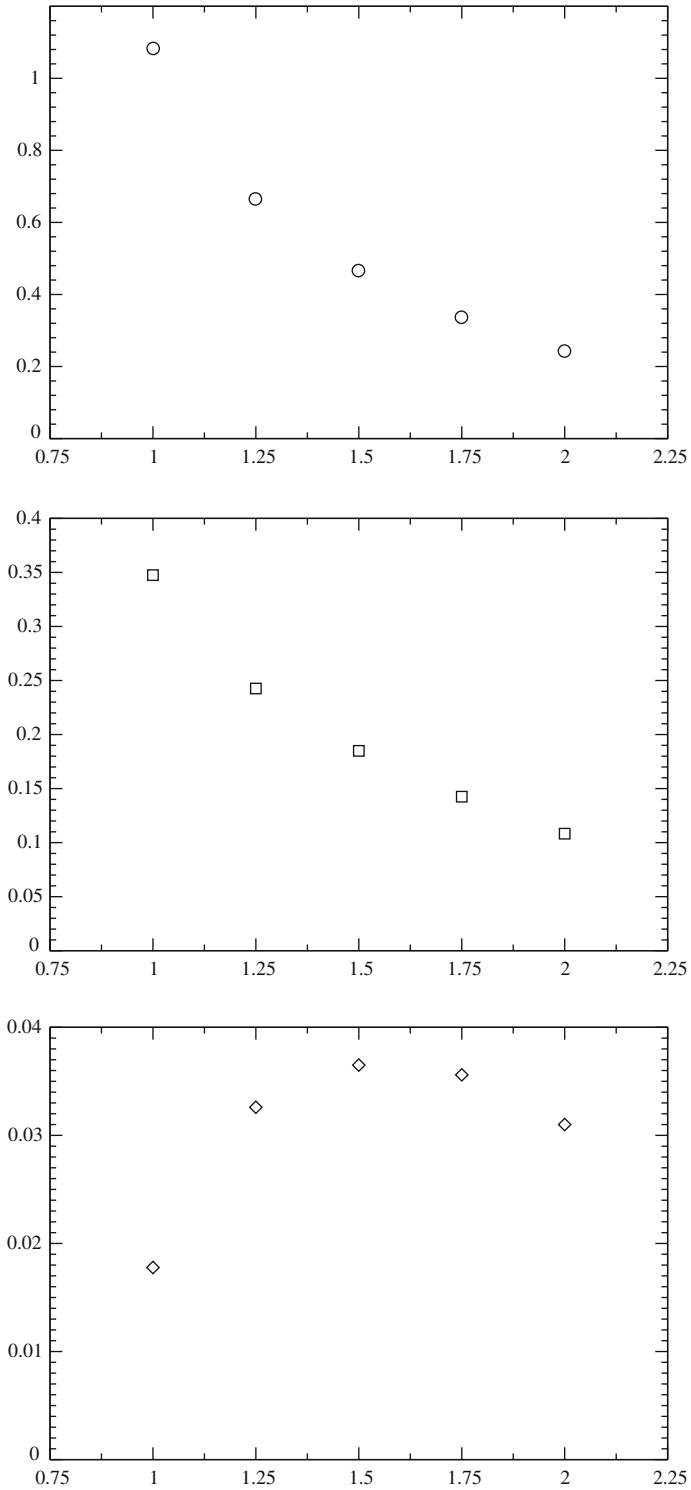

Figure 3. Representation of the numerical results for the probabilistic contribution $(\partial\lambda_p/\partial\mathbf{v})(\partial\mathbf{v}/\partial s)$ scaled by $\partial z/\partial\mathbf{w}$ vs. the scale factor. From top to bottom: $l_c = 15$, 30 and 60 mm.

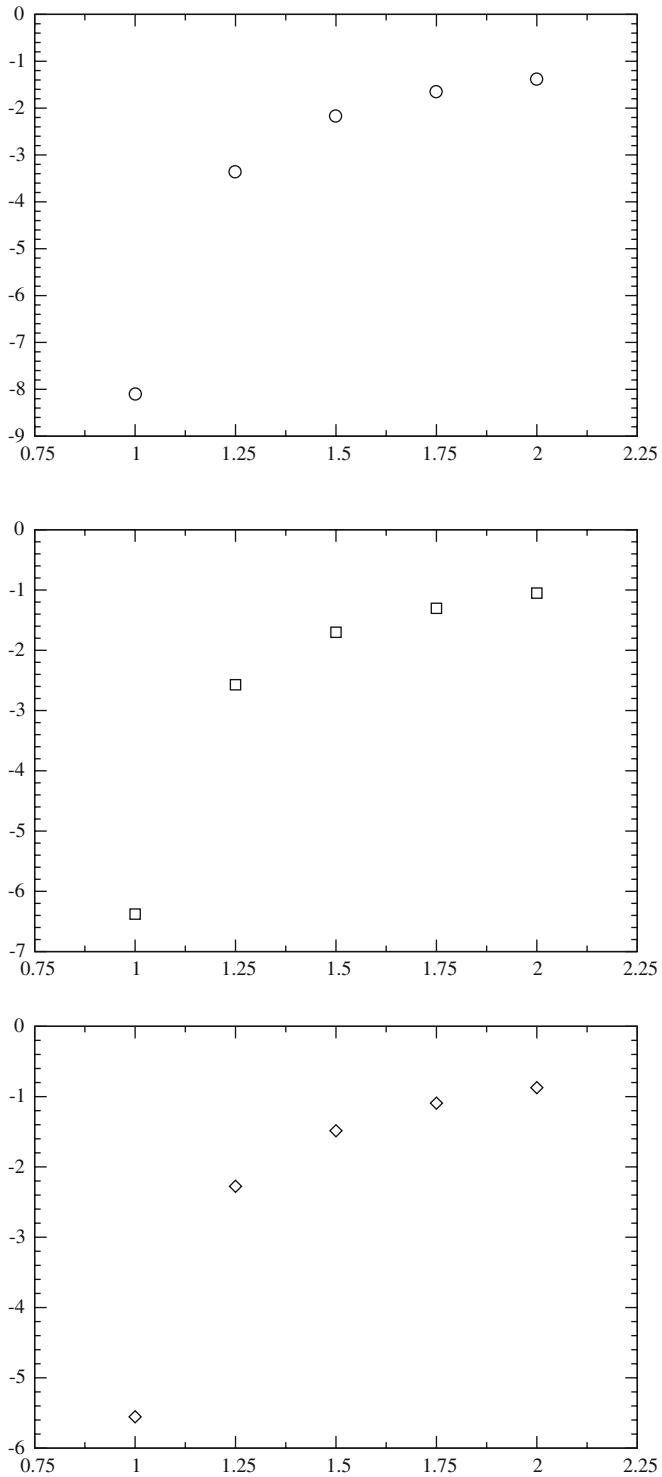

Figure 4. Representation of the numerical results for the deterministic contribution ($\partial\lambda_p/\partial s$) scaled by $\partial z/\partial \mathbf{w}$ vs. the scale factor. From top to bottom: $l_c = 15$, 30 and 60 mm.

6. Conclusions

A method has been presented for direct evaluation of the size sensitivity of the reliability index β. This provides an estimation of the statistical size effect behaviour and of the relative contribution of the involved probabilistic and deterministic phenomena to it. This provides a valuable insight into the actual mechanisms responsible for failure. Indeed, it makes possible to evaluate to which extent the scale factor sensitivity of the failure probability is influenced by phenomena related to the material disorder or the deterministic size effect. This becomes especially relevant when small sizes are considered, because slight absolute size variations manifest themselves as large scale factor variations and because the size sensitivity of the reliability index is larger in such a case. The method is not applicable to large sizes at this stage, because it does not take multiplicity of failure modes into account.

References

Baxter, S.C. and Graham, L.L. (2000). Characterization of random composites using moving-window technique. *Journal of Engineering Mechanics* **126**(4), 389–397.

Bažant, Z.P. and Planas, J. (1998). *Fracture and Size Effect in Concrete and Other Quasibrittle Materials.* CRC Press. Boca Raton, FL.

De Borst, R. (1987). Computation of post-bifurcation and post-failure behaviour of strain-softening solids. *Computers and Structures* **25**, 211–224.

Ditlevsen, O. and Madsen, H.O. (1996). *Structural Reliability Methods.* Wiley, Chichester.

Gutiérrez, M.A. and de Borst, R. (1999). Deterministic and stochastic analysis of size effects and damage evolution in quasi-brittle materials. *Archive of Applied Mechanics* **69**, 655–676.

Gutiérrez, M.A. and de Borst, R. (2000). Stochastic aspects of localised failure: Material and boundary imperfections. *International Journal of Solids and Structures* **37**(48–50), 7145–7159.

Gutiérrez, M.A. and de Borst, R. (2003). Simulation of size-effect behaviour through sensitivity analyses. *Engineering Fracture Mechanics* **70**(16), 2269–2279.

Gutiérrez, M.A. and Krenk, S. (2004). Stochastic finite element methods. In: *Encyclopedia of Computational Mechanics* (edited by E. Stein, R. de Borst and T.J.R. Hughes) Wiley, Chichester, pp. 657–681.

Kleiber, M., Antúnez, H., Hien, T.D. and Kowalczyk, P. (1997). *Parameter Sensitivity in Nonlinear Mechanics.* Wiley, Chichester.

Liu, P.L. and Der Kiureghian, A. (1986). Multivariate distribution models with prescribed marginals and covariances. *Probabilistic Engineering Mechanics* **1**, 105–112.

Liu, P.L. and Der Kiureghian, A. (1991). Optimization algorithms for structural reliability. *Structural Safety* **9**, 161–177.

Peerlings, R.H.J., de Borst, R., Brekelmans, W.A.M. and de Vree, J.H.P. (1996). Gradient enhanced damage for quasi-brittle materials. *International Journal for Numerical Methods in Engineering* **39**, 3391–3403.

Peerlings, R.H.J., de Borst, R., Brekelmans, W.A.M. and Geers, M.G.D. (1998). Gradient-enhanced damage modelling of concrete fracture. *Mechanics of Cohesive-Frictional Materials* **3**, 323–342.

De Vree, J.H.P., Brekelmans, W.A.M. and van Gils, M.A.J. (1995). Comparison of nonlocal approaches in continuum damage mechanics. *Computers and Structures* **55**, 581–588.